An abrupt extinction in the Middle Permian (Capitanian) of the Boreal Realm (Spitsbergen) and its link to anoxia and acidification

David P.G. Bond[1,†], Paul B. Wignall[2], Michael M. Joachimski[3], Yadong Sun[3,4], Ivan Savov[2], Stephen E. Grasby[5,6], Benoit Beauchamp[6], and Dierk P.G. Blomeier[7]

[1]*Department of Geography, Environment and Earth Sciences, University of Hull, Hull, HU6 7RX, United Kingdom*
[2]*School of Earth and Environment, University of Leeds, Leeds, LS2 9JT, United Kingdom*
[3]*Geozentrum Nordbayen, Universität Erlangen-Nürnberg, Schlossgarten 5, 91054 Erlangen, Germany*
[4]*State Key Laboratory of Biogeology and Environmental Geology, China University of Geosciences, 388 Lumo Road, Wuhan, 470073, Hubei Province, P.R. China*
[5]*Geological Survey of Canada, 3303 33rd Street N.W., Calgary, Alberta, T2L 2A7, Canada*
[6]*Department of Geoscience, University of Calgary, 2500 University Drive N.W., Calgary Alberta, T2N 1N4, Canada*
[7]*Norwegian Polar Institute, Fram Centre, 9296 Tromsø, Norway*

ABSTRACT

The controversial Capitanian (Middle Permian, 262 Ma) extinction event is only known from equatorial latitudes, and consequently its global extent is poorly resolved. We demonstrate that there were two, severe extinctions amongst brachiopods in northern Boreal latitudes (Spitsbergen) in the Middle to Late Permian, separated by a recovery phase. New age dating of the Spitsbergen strata (belonging to the Kapp Starostin Formation), using strontium isotopes and $\delta^{13}C$ trends and comparison with better-dated sections in Greenland, suggests that the first crisis occurred in the Capitanian. This age assignment indicates that this Middle Permian extinction is manifested at higher latitudes. Redox proxies (pyrite framboids and trace metals) show that the Boreal crisis coincided with an intensification of oxygen depletion, implicating anoxia in the extinction scenario. The widespread and near-total loss of carbonates across the Boreal Realm also suggests a role for acidification in the crisis. The recovery interval saw the appearance of new brachiopod and bivalve taxa alongside survivors, and an increased mollusk dominance, resulting in an assemblage reminiscent of younger Mesozoic assemblages. The subsequent end-Permian mass extinction terminated this Late Permian radiation.

INTRODUCTION

The Middle Permian (Capitanian Stage) mass extinction is among the least understood of all mass extinction events; it is regarded as either one of the greatest of all Phanerozoic crises, ranking alongside the "Big 5" (Stanley and Yang, 1994; Bond et al., 2010a), or, in a fundamentally different appraisal, it is viewed not as a mass extinction but as a protracted and gradually attained low point in Permian diversity (Yang et al., 2000; Clapham et al., 2009; Groves and Wang, 2013). Until now, all detailed studies have focused on equatorial sections, especially those of South China, where the extinction was first recognized as an especially severe crisis. There, fusulinacean foraminifers and brachiopods lost 82% and 87% of species, respectively (Jin et al., 1994; Shen and Shi, 1996; Bond et al., 2010a). The South China marine losses coincided with the eruption of the Emeishan flood basalt province in the southwest of the country (Fig. 1; Wignall et al., 2009a), supporting a causal link between the two phenomena, but it is unclear if this regional crisis was also a global event. There are several purported kill mechanisms but no consensus, and there are also questions about the nature of the subsequent Late Permian postextinction interval (Bond et al., 2010a). Did marine biota recover from a Capitanian mass extinction (Bond and Wignall, 2009; Wignall et al., 2012) before their final coup-de-grâce in the latest Permian, or did they undergo gradual diversity decline in the run-up to the Permian-Triassic mass extinction, characterized by a slow transition to mixed faunas with Paleozoic and Mesozoic affinities (Clapham and Bottjer, 2007)?

The status and cause of the Capitanian crisis are based on evidence from tropical (Tethyan) latitudes, while little data exist from higher latitudes. Here, we redress this imbalance with a detailed evaluation of Boreal marine fossil ranges in the Kapp Starostin Formation of Spitsbergen, a Permian-aged mixed spiculite chert-carbonate unit that formed in cool, shelf seas of the Boreal Ocean (Ehrenberg et al., 2001; Stemmerik and Worsley, 2005; Blomeier et al., 2013; Dustira et al., 2013). We assess the role of redox changes during this interval using a combination of petrographic and geochemical approaches. The precise age of the formation is unclear, and we investigate this issue with a carbon and strontium isotope chemostratigraphic study and through comparison with better-dated East Greenland successions.

STUDY SECTIONS AND METHODS

We logged and sampled the Kapp Starostin Formation over three field seasons at its eponymous type section near Festningen in central Spitsbergen, and three further sections at Van Keulenhamna, Eholmen, and Forkastningsdalen in southern Spitsbergen (Fig. 2). We examined the Kapp Starostin Formation in the field for its facies and fossil content, identifying the brachiopod and bivalves to genus or species level (see supplemental text: taxonomy[1]), and we took several hundred samples for thin section and geochemical analyses.

The Kapp Starostin Formation consists of Kungurian to latest Permian strata that were deposited on an epicontinental shelf at the northeastern margin of Pangea (Blomeier et al., 2013). This was part of an extensive sea that stretched from Arctic Canada (Sverdrup Basin) and Greenland

[†]d.bond@hull.ac.uk

[1]GSA Data Repository item 2015139, DR1 text (taxonomy), and Figures DR1–DR2, is available at http://www.geosociety.org/pubs/ft2015.htm or by request to editing@geosociety.org.

GSA Bulletin; September/October 2015; v. 127; no. 9/10; p. 1411–1421; doi: 10.1130/B31216.1; 8 figures; 1 table; Data Repository item 2015139; published online 14 April 2015.

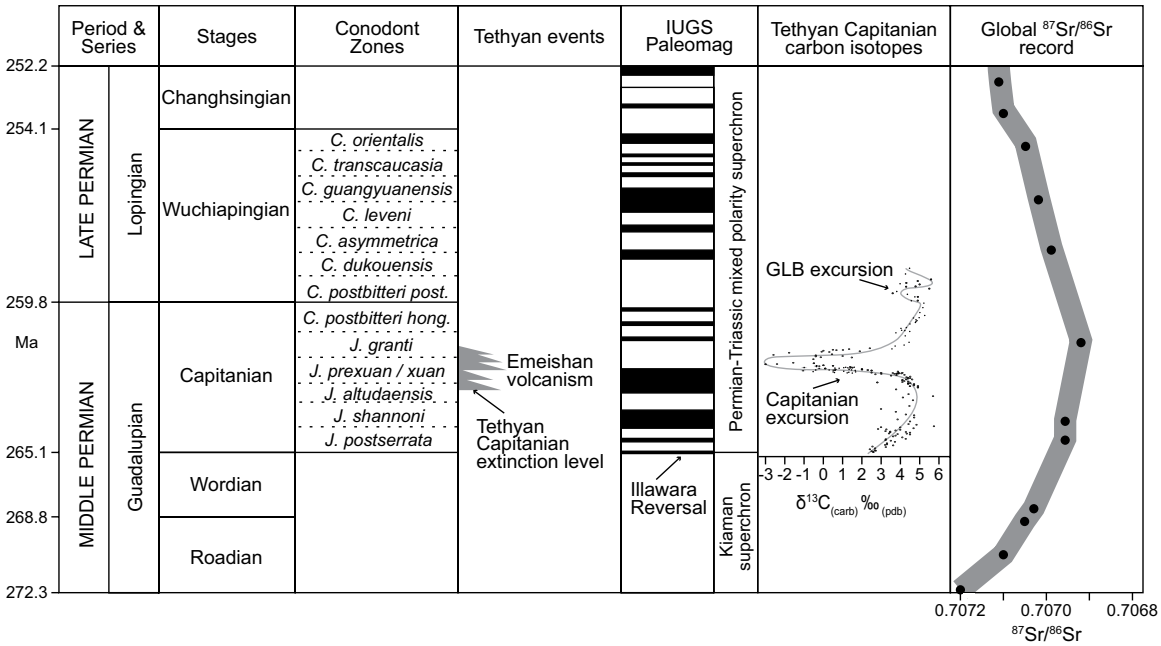

Figure 1. Summary of Middle to Late Permian stratigraphy, Capitanian and Wuchiapingian conodont zones, the Tethyan $\delta^{13}C_{carb}$ record (after Wang et al., 2004; Bond et al., 2010b), the global $^{87}Sr/^{86}Sr$ curve (from Korte et al., 2006), and the International Union of Geological Sciences (IUGS) paleomagnetostratigraphic "bar code," in which periods of normal and reversed polarity are shown as black and white intervals respectively. Ages of stage boundaries after Cohen et al. (2013). Placement of the Illawara reversal is after Isozaki (2009). Abbreviations for conodont zones and stage names as follows: *J.—Jinogondolella*; *C.—Clarkina*; *prexuan/xuan—prexuanhanensis/xuanhanensis*; *hong—hongshuensis*; *post—postbitteri*; GLB—Guadalupian/Lopingian boundary. The timing of Emeishan volcanism and the low-latitude Capitanian mass extinction is based on Wignall et al. (2009a). pdb—Peedee belemnite.

(Wandel Sea Basin) in the west, through Svalbard and the Barents Sea (Finnmark Platform, Stappen High), to Russia (Timan-Pechora Basin) in the east (Stemmerik and Worsley, 2005). The shelf was located at ~45°N in the Middle to Late Permian. The Kapp Starostin Formation contains cool-water Boreal faunas that include abundant siliceous sponges, brachiopods, and bryozoans (e.g., Gobbett, 1964; Kobayashi, 1997; Shen and Shi, 2004). The formation attains its greatest thickness in central Spitsbergen, where it reaches >400 m thick, and thins southwards, eventually pinching out at the Sørkapp-Hornsund High (Dallmann, 1999). We logged and sampled the upper ~220 m in the southern locations, and the upper 90 m at Kapp Starostin (Figs. 3 and 4; supplemental Fig. DR1 [see footnote 1]).

Chemostratigraphy

Tethyan $\delta^{13}C$ records reveal distinctive, probably global, trends in the carbon isotopic composition of Middle to Late Permian seawater. The Capitanian extinction is associated with a –6‰ $\delta^{13}C_{carb}$ excursion in Tethys that coincides with the onset of Emeishan large igneous province volcanism in the *Jinogondolella altudaensis* conodont zone (Fig. 1; Wignall et al., 2009a). A younger and smaller negative shift in $\delta^{13}C_{carb}$ is also known from the Capitanian-Wuchiapingian Stage boundary (the Guadalupian-Lopingian Series boundary; Fig. 1) in China and Japan (Fig. 1; Wang et al., 2004; Isozaki et al., 2007). The Middle to Late Permian $\delta^{13}C$ chemostratigraphic record can be compared with the $^{87}Sr/^{86}Sr$ record of Permian seawater that derives from brachiopod shells (McArthur et al., 2001; Korte et al., 2006). The $^{87}Sr/^{86}Sr$ values decline to a Phanerozoic low point of ~0.70685 in the late Capitanian (Fig. 1; Korte et al., 2006). This has been attributed to minimal runoff of radiogenic Sr from the highly arid Pangean supercontinent (Gibbs et al., 1999). Together, the C and Sr isotopic records provide a chemostratigraphic scheme to help better constrain the Permian strata of Spitsbergen.

We generated three independent carbon isotope ($\delta^{13}C_{org}$) curves through the Kapp Starostin Formation (Fig. 3) according to the following methods: In Calgary (curve of S. Grasby), $\delta^{13}C_{org}$ was measured using continuous flow–elemental analysis–isotope ratio mass spectrometry, with a Finnigan Mat Delta+XL mass spectrometer interfaced with a Costech 4010 elemental analyzer, with standards run every fifth sample. Combined analytical and sampling error for $\delta^{13}C_{org}$ is ±0.2‰ (1σ). In Erlangen (curves of M. Joachimski and Y. Sun), $\delta^{13}C_{org}$ was determined with an elemental analyzer (CE 1110) connected online to a ThermoFisher Delta V Plus mass spectrometer, and accuracy and reproducibility of the analyses were checked by replicate analyses of international (USGS 40) or laboratory standards. Reproducibility of replicate standard analyses was ±0.07‰ (1σ). Values are reported in conventional δ notation in permil relative to Vienna Peedee belemnite (V-PDB).

Our Boreal strontium isotope record was generated from brachiopod shells screened using cathodoluminescence (Fig. 3; supplemental Fig. DR2 [see footnote 1]). Powdered samples were screened on the University of Leeds Philips PW1050 X-ray diffractometer (XRD), which revealed the presence of only pure calcite and quartz. Atomic absorption spectroscopy measurements for Ca, Mg, Sr, Mn, and Fe revealed elemental abundances resembling carbonates from shells in equilibrium with modern ocean

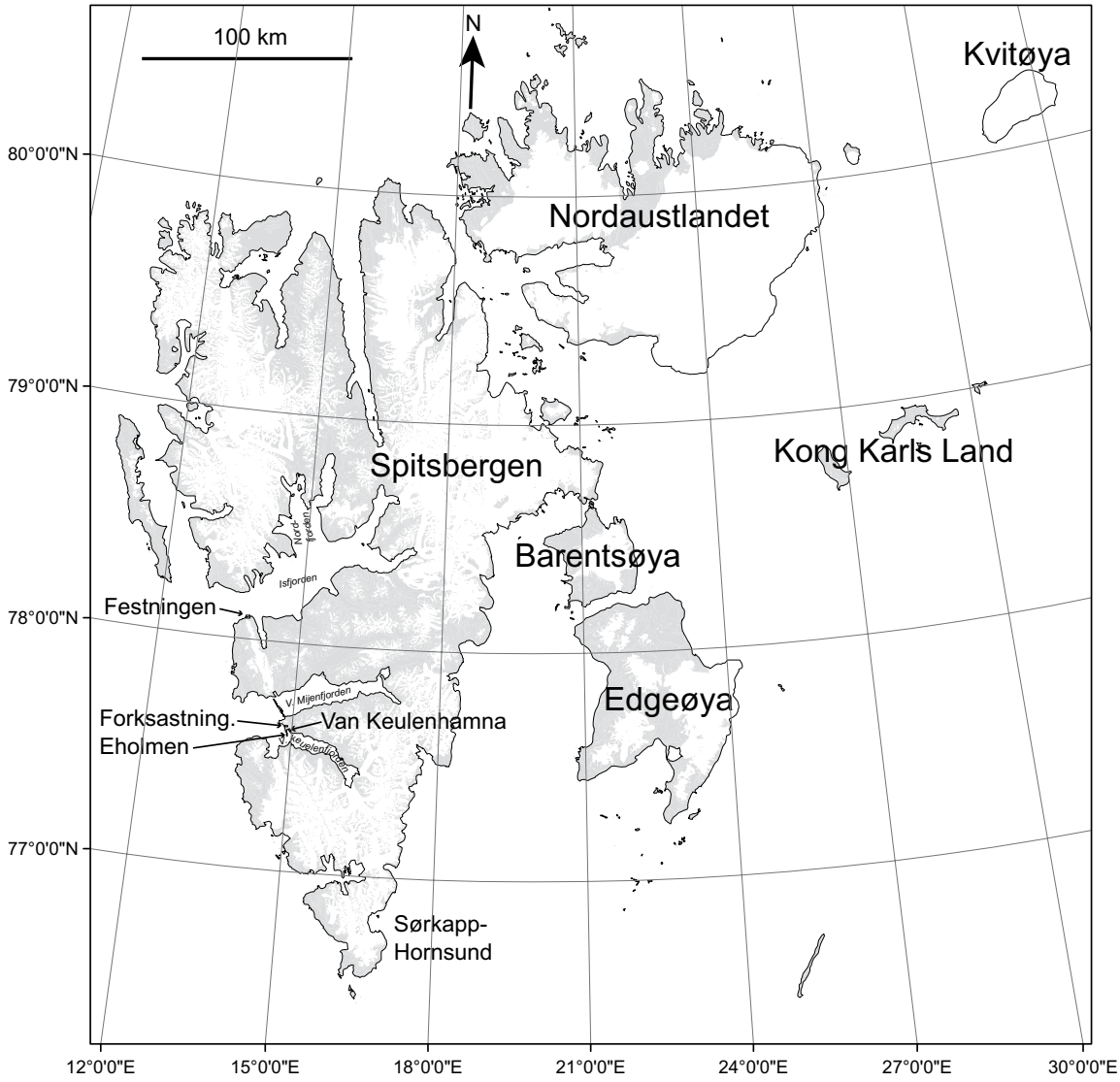

Figure 2. Map of Svalbard showing the major islands and the location of the four study sections. Shaded areas are bedrock exposures. White areas are glaciated. Base map was provided by W.K. Dallmann of the Norwegian Polar Institute. Forkastning.—Forkastningsdalen.

waters. Subsequent $^{87}Sr/^{86}Sr$ measurements were performed by I. Savov at the Thermal Ionization Mass Spectrometry Laboratory in Leeds. Carbonate powders underwent the leaching procedure described by McArthur et al. (2000). Evaporated Sr extracts were re-dissolved in ultrapure weak HCl and added onto tungsten wire with a previously applied 5% $TaCl_5$ solution (to ease ionization). The $^{87}Sr/^{86}Sr$ ratios were measured on a Thermo-Scientific Triton-series thermal ionization mass spectrometer. Internal precision was maintained between 5 and 13×10^{-6} (at 2σ). Analytical precision was monitored by repeated analysis of the standard NBS-987. During analysis, the mean measured value obtained for NBS-987 was 0.710272 ± 0.000011 (2σ, $n = 17$). All reported $^{87}Sr/^{86}Sr$ data were normalized to the NBS-987 literature value of 0.710248. Total blanks were ~300 pg Sr. The concentrations of Rb in calcite shells were too low to require correction for radiogenic (^{87}Sr) in-growth. The $^{87}Sr/^{86}Sr$ ratios were normalized for mass fractionation to $^{86}Sr/^{88}Sr = 0.1194$.

Redox Proxies

Pyrite framboid analysis is a powerful tool for reconstructing ancient redox conditions. In modern environments, pyrite framboids form in the narrow iron-reduction zone developed at the redox boundary, but they cease growing in the more intensely anoxic conditions of the underlying sulfate-reduction zone (Wilkin et al., 1996; Wilkin and Barnes, 1997; Suits and Wilkin, 1998). If bottom waters become euxinic (i.e., free H_2S occurs within the water column), then framboids develop in the water column but are unable to achieve diameters much larger than 5–6 μm before they sink below the iron reduction zone and cease to grow (Wilkin et al., 1996). Thus, euxinic conditions are characterized by populations of tiny framboids with a narrow size range. In contrast, dysoxic or weakly oxygenated seafloors produce framboid populations that are larger and more variable in size, because their growth is restricted only by the local availability of reactants (Wilkin et al., 1996; Bond and Wignall, 2010).

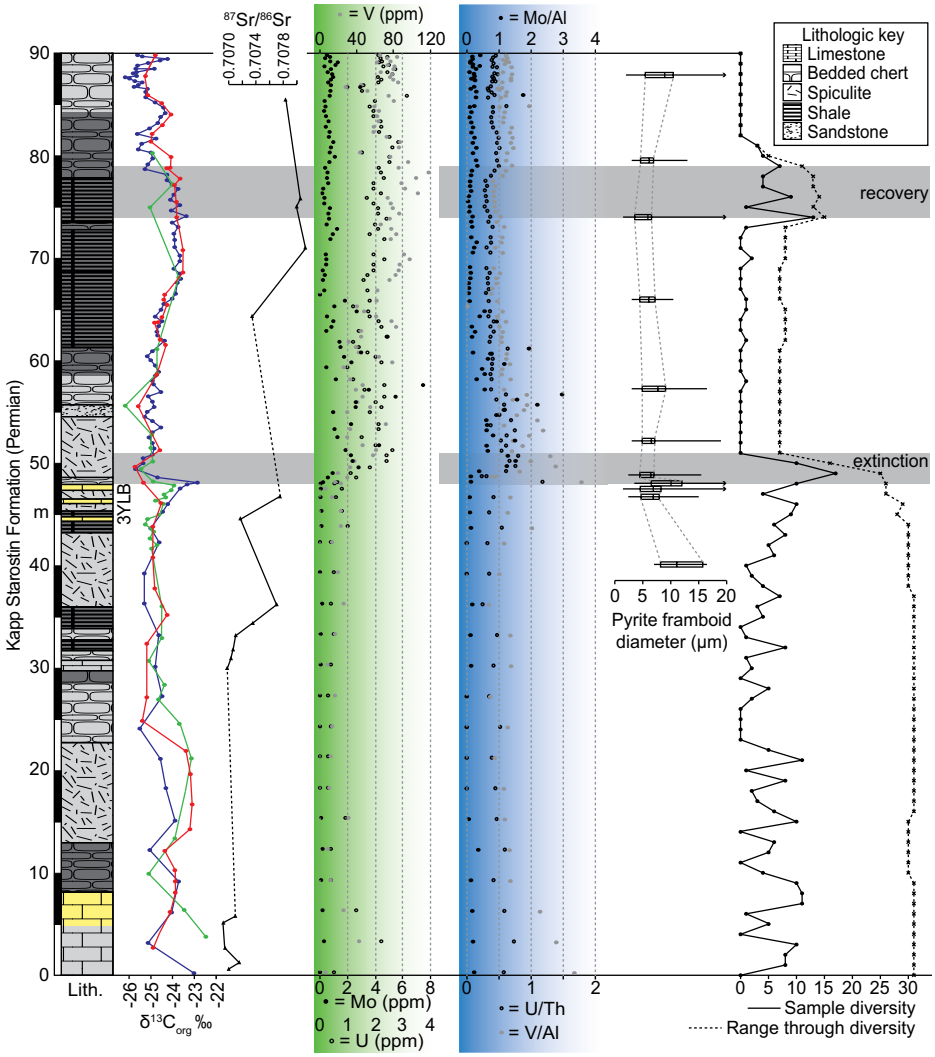

Figure 3. Log of the Kapp Starostin section (78.0950°N, 13.8240°E [WGS84 datum]) showing the upper part of the Kapp Starostin Formation up to the contact with the overlying Vardebukta Formation at 90 m height. Colors in the lithology column indicate pale gray, dark gray, and yellow beds (3YLB—three yellow limestone beds used for correlation between sections). Three separate organic carbon isotope ($\delta^{13}C_{org}$) curves were generated by M. Joachimski (red circles), Y. Sun (green circles), and S. Grasby (blue circles). All three curves are in excellent accord. The $^{87}Sr/^{86}Sr$ curve (black triangles) was generated from brachiopod shells: Low values in the lower part of the section are consistent with the Middle Permian low point of the global curve (Korte et al., 2006; see Fig. 1). The marked increase to more radiogenic values in the postextinction interval is suggestive of a Late Permian age for the upper part of the section, although the extremely high values in the topmost part of the section suggest diagenetic overprinting. Elemental concentrations of trace metals (green shaded box) show an enrichment in molybdenum (Mo, black circles), uranium (U, open circles), and vanadium (V, gray circles) in the extinction interval, suggesting anoxic conditions developed at Kapp Starostin in the Middle to Late Permian. Normalized trace metal analyses (blue shaded box) (Mo/Al, U/Th, V/Al) suggest that the enrichment in redox-sensitive metals is independent of facies/terrigenous input. Pyrite framboid box and whisker plots show the 25th and 75th percentiles of framboid diameters in each sample (horizontal extent of black box), mean framboid diameter (central vertical line), and maximum and minimum framboid diameter (long horizontal line). The diversity curve (diversity taken from the composite log in Fig. 7) depicts the number of brachiopod and bivalve taxa (circles and solid line). Range-through (standing) diversity (including taxa known to be extant at each level) is shown as crosses and dashed line. Mass extinction and recovery intervals are shaded gray.

Field samples from Kapp Starostin and Van Keulenhamna were examined by P. Wignall using gold-coated polished chips viewed in backscatter mode at 2500× magnification under an FEI Quanta 650 FEG-ESEM scanning electron microscope to determine pyrite content, and, where present, the size distribution of pyrite framboids (Fig. 3). Where possible, at least 100 framboids were measured from each sample. Framboid size distributions are plotted with mean diameter versus standard deviation within each sample, which allows comparison of framboid populations in ancient sediments with modern euxinic, anoxic, and dysoxic populations.

The concentrations of redox-sensitive trace metals in marine sediment provide an additional measure of ancient depositional conditions, because the reduced forms of many metals (e.g., molybdenum, uranium, and vanadium) are insoluble in seawater, with the result that these elements are scavenged by sediment under anoxic conditions.

Determinations of U, Mo, and V concentrations were performed by S. Grasby at the Isotope Science Laboratory, University of Calgary, using the same samples that were taken for $\delta^{13}C_{org}$ analysis. Elemental determinations were conducted on powdered samples digested in a 2:2:1:1 acid solution of H_2O-HF-$HClO_4$-HNO_3 and subsequently analyzed using a PerkinElmer mass spectrometer with ±2% analytical error. Our normalized trace metal data (Mo/Al, V/Al, and U/Th) confirm that fluctuations in trace metal concentrations were due to redox changes and not related to variations in carbonate content, because the major shift in values occurs within a spiculitic chert unit. We found excellent accordance between the redox history interpreted from pyrite framboid distributions and that inferred from trace metal concentrations.

RESULTS

Toward an Age Model

Our three independent organic carbon isotope curves for the Kapp Starostin Formation are in close accord and reveal relatively high $\delta^{13}C_{org}$ values in the central part of the Kapp Starostin Formation, before an ~3‰ negative shift at a level marked by three, distinctive brachiopod-rich yellow limestone beds (hereafter called the "3YLB" level) beginning ~44 m beneath the top of the formation at Kapp Starostin. The $\delta^{13}C_{org}$ low point is followed by a gradual, rising trend (Fig. 3). A $\delta^{13}C_{org}$ record is not available from Tethyan locations for comparison, but several $\delta^{13}C_{carb}$ studies in the region show a similar (albeit often larger, at around 6‰) negative excursion that began in the middle Capita-

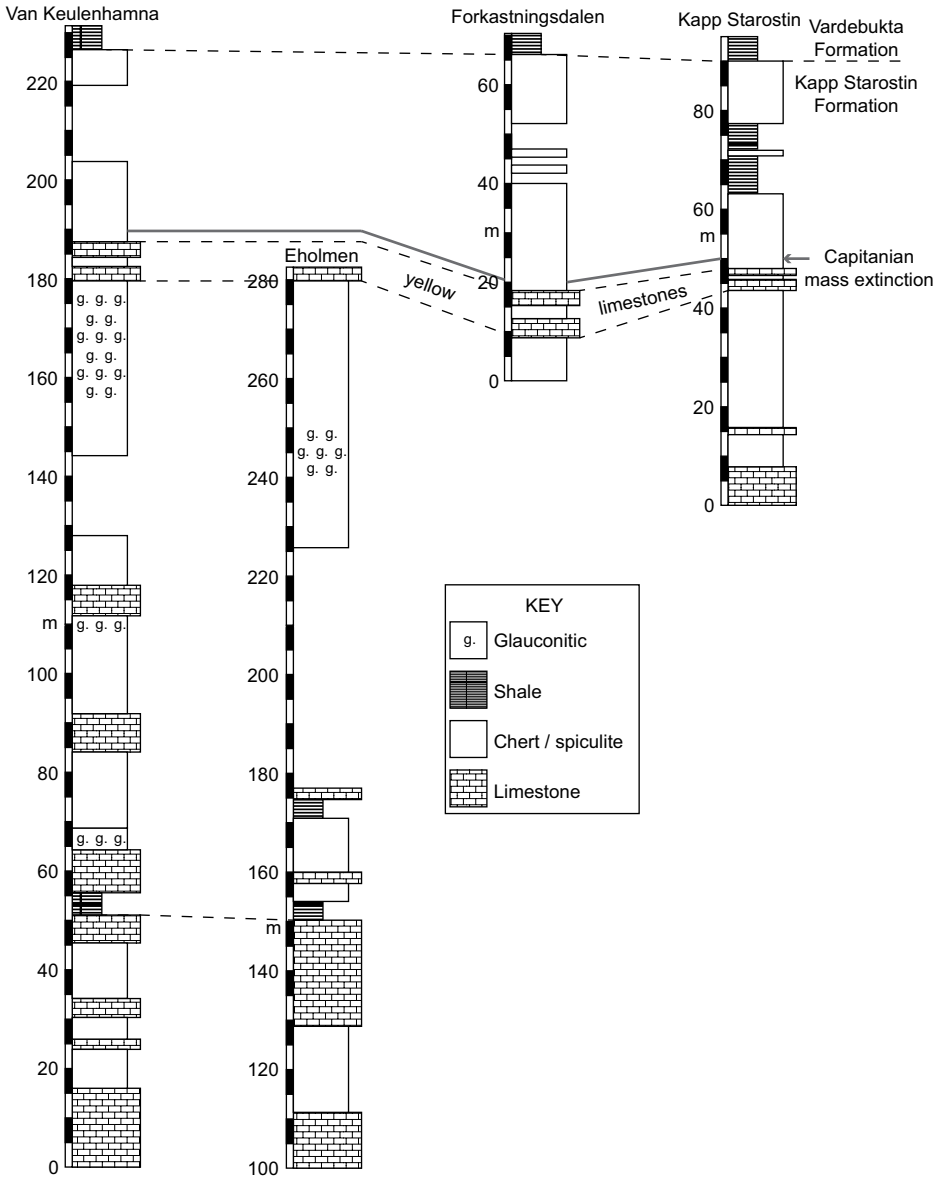

Figure 4. Correlation panel with simplified lithologic logs from Kapp Starostin (78.0950°N, 13.8240°E [WGS84 datum]), Van Keulenhamna (77.6102°N, 14.9706°E [WGS84]), Eholmen (77.5982°N, 14.9146°E [WGS84]), and Forkastningsdalen (77.6427°N, 14.9041°E [WGS84]). The three yellow limestone beds (3YLB) that immediately precede the extinction horizon have been used to correlate between sections.

nian *Jinogondolella altudaensis* conodont zone (e.g., Bond et al., 2010b; Fig. 1). We note that some studies do not find this negative excursion, perhaps due to the presence of hiatuses (Jost et al., 2014).

The marine Permian $^{87}Sr/^{86}Sr$ record shows a decline to a low of 0.70685 in the middle to late Capitanian, followed by a rapid rise to values of 0.7075 at the Permian-Triassic boundary (McArthur et al., 2001; Korte et al., 2006; Kani et al., 2008, 2013; Fig. 1). Our record from Spitsbergen shows a similar low point, followed by a rising trend: We see values of 0.7069 around 90 m below the top of the Kapp Starostin Formation before a two-stage rise, first to ~0.7073 some 55 m below the formation top, and more substantially to values of 0.7080 in the topmost meters (Fig. 3). This pattern is closely comparable to the most detailed previously published Sr record from the Kapp Starostin Formation of Gruszczynski et al. (1992). Our uppermost Kapp Starostin Formation values are radiogenically enriched in comparison to usual Late Permian values, suggesting that our youngest brachiopod samples have undergone diagenetic alteration and do not yield reliable data. Nevertheless, the $^{87}Sr/^{86}Sr$ low point recorded in the lower part of the section (90–55 m below the top of Kapp Starostin Formation) shows a good match to global data sets and provides some support for a middle Capitanian age for this level in the formation. This interpretation is in accordance with recent attempts at Sr dating of the Kapp Starostin Formation by Ehrenberg et al. (2010), who assigned a Roadian to Capitanian age to its upper half.

The combined $\delta^{13}C_{org}$ and $^{87}Sr/^{86}Sr$ records both suggest a middle Capitanian age for a level high in the Kapp Starostin Formation near the 3YLB. Paleomagnetic evidence also supports this age assignment. The strata in western Isfjorden (Fig. 2) have undergone partial remagnetization, but the primary magnetostratigraphic signal shows a switch from normal to reversed polarities ~40 m from the top of the formation—a change that suggests an end-Capitanian age (Nawrocki and Grabowski, 2000; Hounslow and Nawrocki, 2008). Taken together, the carbon isotope, strontium isotope, and paleomagnetic evidences all suggest that the 3YLB level in the Kapp Starostin Formation is of intra-Capitanian age. In the absence of biostratigraphically useful fossils within the formation, this age designation must remain a compelling but unproven hypothesis.

The age of the topmost 40 m of the Kapp Starostin Formation is also rather equivocal. Considered to be latest Permian by most authors, there is debate as to whether the latest Permian Changhsingian Stage is missing (Nawrocki and Grabowski, 2000; Hounslow and Nawrocki, 2008) or whether the entire Late Permian is complete, at least in the expanded sections of western Spitsbergen such as Kapp Starostin (Wignall et al., 1998).

Intra-Permian Extinction and Recovery

The 3YLB level forms a distinctive, correlatable horizon in all of our studied locations, together with other brachiopod- and bryozoan-rich limestone beds present at lower levels (Fig. 4). This allows faunal ranges from individual sections to be compiled onto a single chart. We focused our analysis on brachiopods and bivalves of the uppermost two thirds of the Kapp Starostin Formation (supplemental information: Taxonomy [see footnote 1]; Figs. 5 and 6). This reveals an abundant and diverse brachiopod-dominated assemblage with stable diversity and composition throughout much of the Kapp Starostin Formation, as originally noted in the detailed study of Gobbett (1964). This stability was sharply terminated immedi-

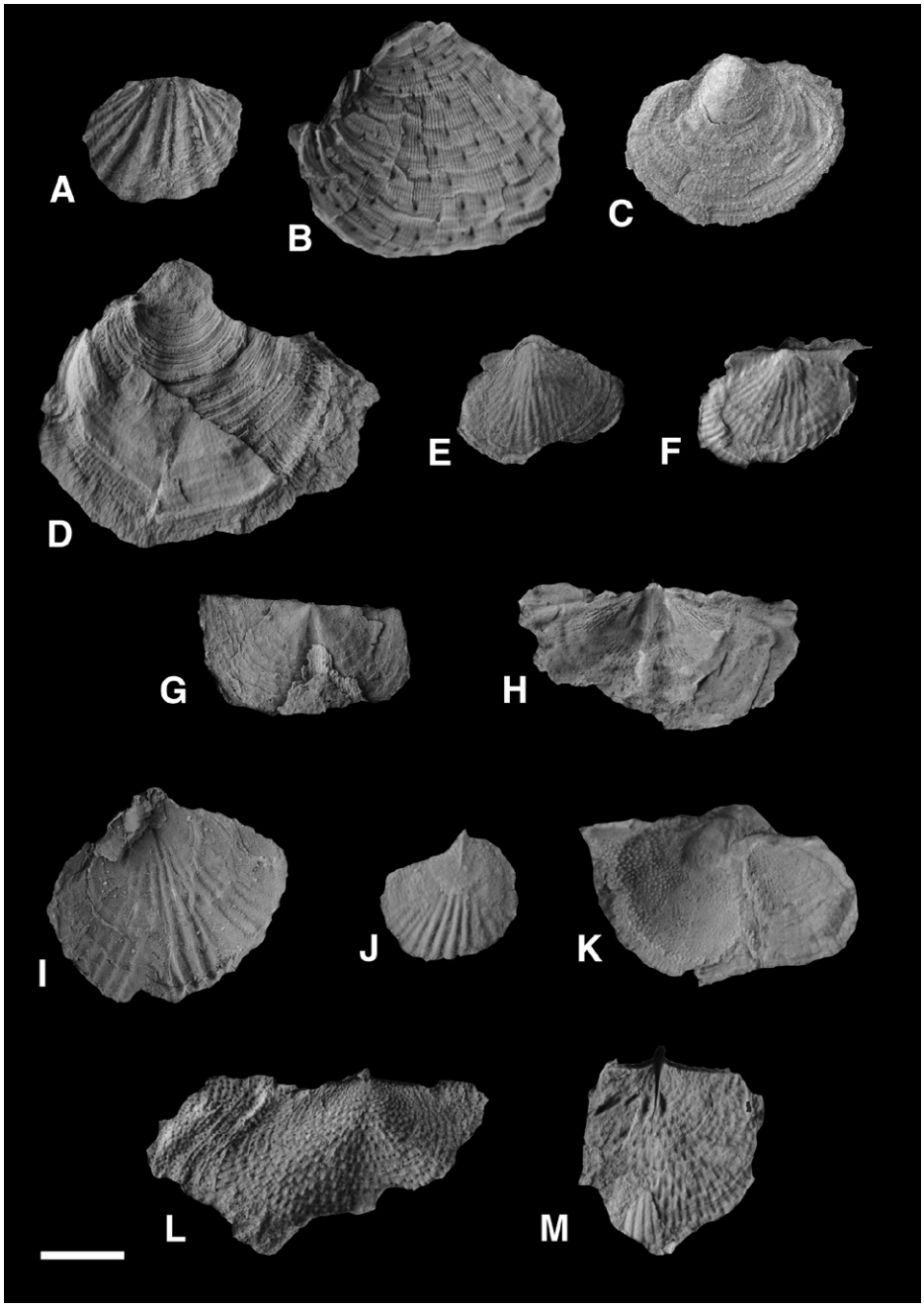

Figure 5. Brachiopods from the Kapp Starostin Formation at Kapp Starostin. (A) *Brachythyrina* sp.; (B) *Cancrinella spitsbergiana*; (C, D) indet. echinochoncids; (E, F) *Haydenella* sp.; (G) *Lissochonetes superba*; (H) *Lissochonetes superba* showing papillose areas either side of the centrum; (I, J) *Stenocisma* sp. 2; (K, L, M) *Waagenoconcha* sp. Scale bar is 1 cm.

ately above the 3YLB, when 87% (28 of 32) of brachiopod species and two out of four bivalve species disappear within a 30-cm-thick section of dark spiculitic chert (Figs. 3 and 7; supplemental Fig. DR1 [see footnote 1]).

The extinction removed many common Kapp Starostin Formation species (Figs. 3 and 7; supplemental Fig. DR1 [see footnote 1]), including *Bruntonia maynci*, *Dyoros (Dyoros) spitzbergianus*, *Kuvelousia weyprechti*, *Paeckelmania* sp., *Paraspiriferina* sp., *Tumarina* sp., *Fasiculatia striatoplicatus*, *Krotovia* sp., *Anemonaria* sp., *Rhynchopora variabilis*, *Spiriferella* spp., *Svalbardoproductus* sp., *Chaoiella* sp., *Composita* sp., *Kochiproductus* sp., *Derbyia grandis*, *Thuleproductus* sp., *Cleiothyridinia* sp., *Bathymyonia* sp., *Cancrinella* sp., and *Dielasma* cf. *plica*. Only *Waagenoconcha* sp., *Liosetella hemispherica* sp., *Lingula freboldi*, and *Stenocisma* sp. nov. survived the cull (Fig. 7).

Following the extinction, younger Permian fossils are found in a series of shale-dominated horizons interbedded with barren cherts (Figs. 3 and 7; supplemental Fig. DR1 [see footnote 1]). These shales are exposed at Kapp Starostin but covered in the other study sections. The youngest Kapp Starostin Formation fauna consists of a few pre-extinction and several new brachiopod species, which include *Stenocisma* sp. nov. 2, *Spiriferella keilhavii*, *Dyoros. (D.) mucronata*, an indet. echinoconchid, *Lissochonetes superba*, *Rhynchopora kochi*, and *Cancrinella spitsbergiana*, and new bivalve species including *Grammatodon* (*Cosmetodon*)? *suzuki*, *Palaeolima* sp., *Atomodesma* sp. 1, and *Atomodesma* sp. 2. Bivalves suffered a lower proportion of losses across the extinction horizon relative to brachiopods, and this group constitutes a greater proportion of postextinction fossil assemblages (7 bivalves out of 15 bivalve and brachiopod taxa present, in contrast to 8 out of 40 pre-extinction taxa). Bryozoans also are abundant at this level, although their diversity is considerably reduced compared with the fauna below the first extinction horizon (Ezaki et al., 1994).

This new postextinction fauna persists through only ~10 m of strata before it disappears 10 m below the top of the Kapp Starostin Formation (Fig. 7). This level may occur in either the early Late Permian Wuchiapingian Stage or within the subsequent Changhsingian Stage. Further work is needed to better date this second extinction. A third extinction occurs at the top of the Kapp Starostin Formation, where siliceous sponges together with the soft-bodied infauna responsible for abundant trace fossils disappear. This final extinction is associated with a major negative carbon isotope excursion and is considered to be the end-Permian mass extinction (Wignall et al., 1998; Dustira et al., 2013).

Redox Changes

Elemental concentrations of U, V, and Mo as well as normalized values (U/Th, Mo/Al, and V/Al) are presented in Figure 3. Concentrations of these redox-sensitive trace metals are low throughout the Kapp Starostin Formation but rise at the first extinction level and remain high in the succeeding barren interval (Fig. 3). The diverse recovery fauna coincides with a decline of Mo values, but other trace metal concentrations remain stable—perhaps a subtle indicator of improved ventilation and a function of the greater enrichment of U in dysoxic waters

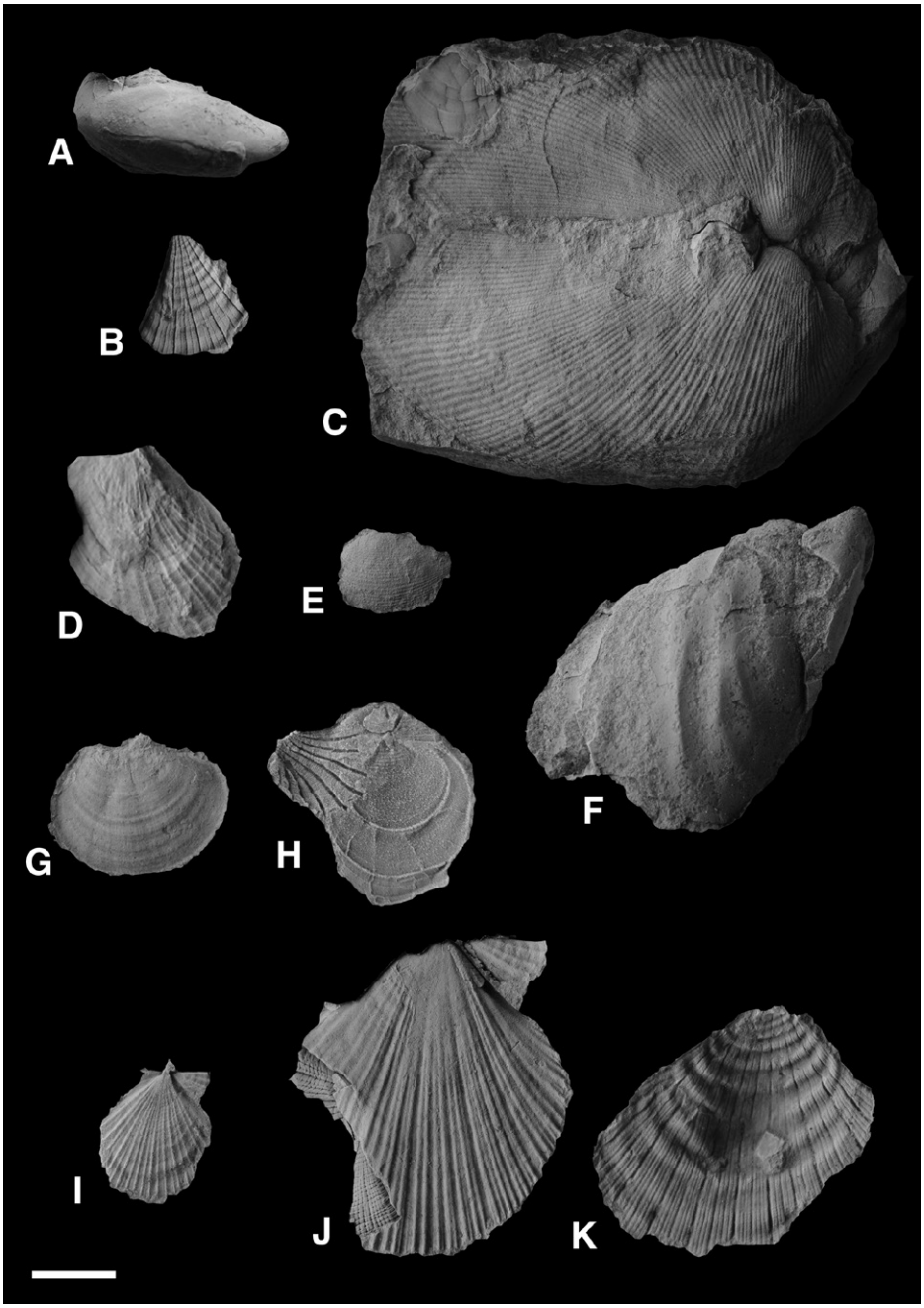

Figure 6. Bivalves from the Kapp Starostin Formation at Kapp Starostin. (A) Indet. buchid; (B) *Etheripecten keyslingiformis*; (C) *Grammatodon* (*Cosmetodon*)? *suzuki*; (D) *Palaeolima* sp.; (E) *Palaeoneilo* sp.; (F) *Retroceramus* sp.; (G) *Streblopteria winsnesi*; (H) *Streblopteria winsnesi* overlain by a fragment of *Cassianoides*; (I, J) *Vorkutopecten svalbardensis*; (K) *Vorkutopecten* sp. Scale bar is 1 cm.

relative to Mo, which only becomes enriched in sulfidic waters (Zhou et al., 2012).

Pyrite framboid analysis supports the redox history inferred from the trace metal trends. In the Kapp Starostin section, larger framboids with a wider size distribution (greater standard deviation) reveal weakly dysoxic conditions prior to the extinction. This is followed by a reduction in mean framboid diameters (and standard deviation) at the extinction level, indicating euxinic conditions (Table 1; Figs. 3 and 8). Framboids remain small until near the top of the Kapp Starostin Formation at Kapp Starostin. In contrast, the Kapp Starostin Formation strata from southern Spitsbergen (e.g., Van Keulenhamna) contain few pyrite framboids, suggesting development of much weaker dysoxia in this area.

DISCUSSION

A Capitanian Extinction in Boreal Latitudes?

Our Spitsbergen study reveals two shelly invertebrate extinction levels in the upper Kapp Starostin Formation. Most losses occurred during the first extinction, which was especially severe for the dominant brachiopod fauna, of which 87% of species disappear within a few tens of centimeters of strata. This extinction level is considered to occur within the Capitanian Stage, based on the multiple lines of evidence discussed herein, and so it provides the first evidence for a mass extinction of this age in higher latitudes. It is noteworthy that the brachiopod losses are similar to those suffered by brachiopods in South China, where 87% of species were also lost (Shen and Shi, 1996). Published range data on bryozoans and rugose corals in the Kapp Starostin Formation are of low resolution (Ezaki and Kawamura, 1992; Ezaki et al., 1994; Nakrem, 1994), but their diversity is much reduced in the upper 40 m of the formation, suggesting that these groups also suffered a Capitanian extinction.

The occurrence of a Boreal mass extinction in the Capitanian is also supported by comparison with the published marine fossil record from East Greenland, which was situated ~1500 km to the south of Spitsbergen during the Permian, although here too the age assignments are controversial. The youngest Permian strata in East Greenland consist of the Wegener Halvø Formation and the overlying Schuchert Dal Formation (Stemmerik, 2001). The Wegener Halvø Formation contains abundant and diverse brachiopods and bryozoans that share many taxa with the Kapp Starostin Formation (Dunbar, 1955). The majority of these taxa disappear at the top of the formation, and the overlying Schuchert Dal Formation fauna is both rare and of low diversity (Sørensen et al., 2007). However, there are reworked blocks of white limestone present in the lowest Triassic that have been eroded from a latest Permian unit not seen in outcrop (Dunbar, 1955). The white blocks contain a diverse and distinct fauna of brachiopods and bivalves that is remarkably similar to the distinctive postextinction assemblages of the Kapp Starostin Formation in Spitsbergen, and includes *Rhynchopora kochi*, *Grammatodon* spp., and atomodesmatids (Dunbar, 1955). Thus, the East Greenland fossils reveal a very similar history to those from Spitsbergen, with major diversity losses

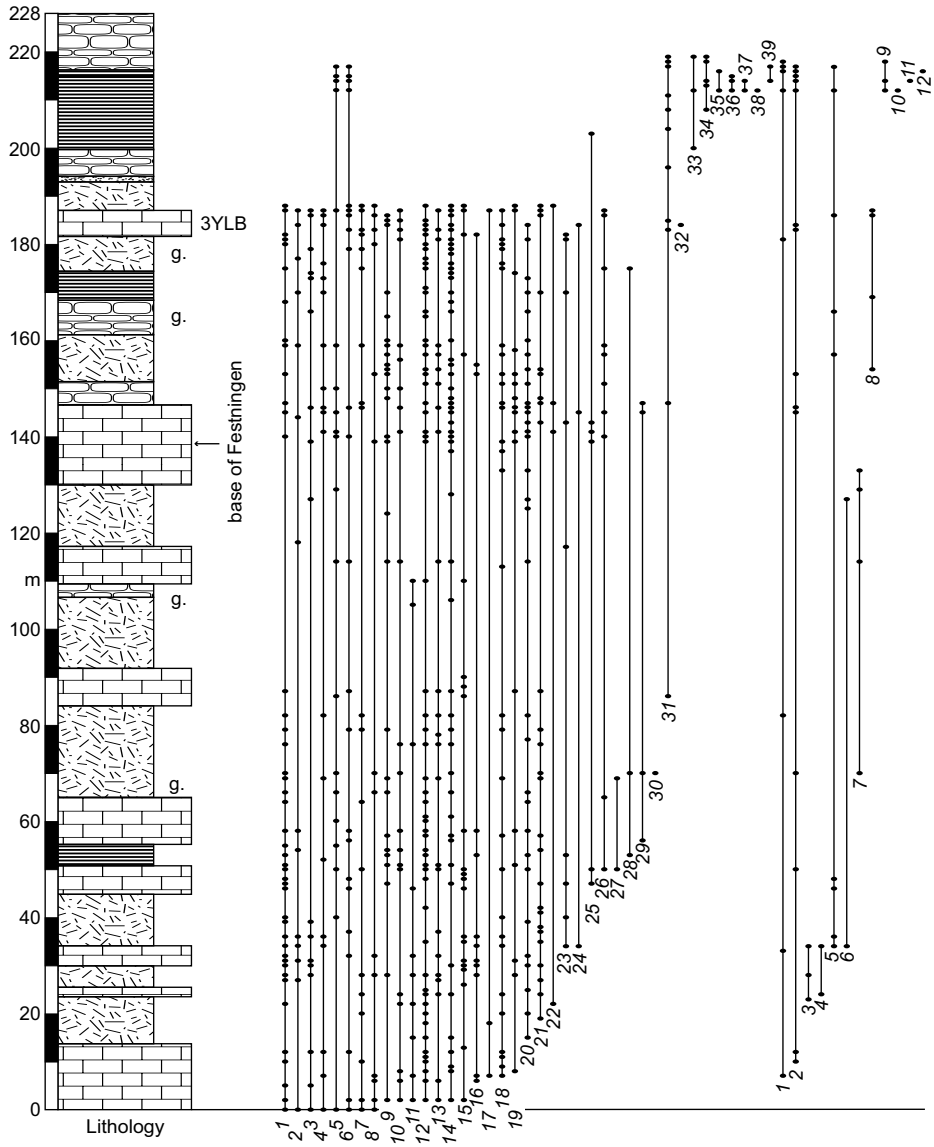

Figure 7. Composite brachiopod (1–39) and bivalve (1–12) range chart from the studied sections spanning the top 228 m of the Kapp Starostin Formation. The base of the studied section at Festningen (Fig. 3) is marked at 138 m height on the composite log. The top of this log at 228 m height marks the contact between the Kapp Starostin Formation and overlying Vardebukta Formation. Levels marked "g." are glauconitic. "3YLB" marks the position of the three yellow limestone beds that have been used for correlation and immediately precede the mass extinction. The key for lithologic symbols is given in Figure 3. Brachiopod taxa (left): 1—*Bruntonia maynci*; 2—*Dyoros (Dyoros) spitzbergianus*; 3—*Kuvelousia weyprechti*; 4—*Paeckelmania* sp.; 5—*Waagenoconcha* sp.; 6—*Liosetella hemispherica* sp.; 7—*Paraspiriferina* sp.; 8—*Tumarina* sp.; 9—*Fasiculatia striatoplicatus*; 10—*Krotovia* sp.; 11—*Linoproductus* sp.; 12—*Anemonaria* sp.; 13—*Rhynchopora variabilis*; 14—*Spiriferella* spp.; 15—*Svalbardoproductus* sp.; 16—*Chaoiella* sp.; 17—*Composita* sp.; 18—*Kochiproductus* sp.; 19—*Derbyia grandis*; 20—*Thuleproductus* sp.; 21—*Cleiothyridinia* sp.; 22—*Bathymyonia* sp.; 23—*Cancrinella* sp.; 24—*Dielasma* cf. *plica*; 25—*Lingula freboldi*; 26—*Archboldia impressa*; 27—*Orbiculoidea winsnesi*; 28—*Liosotella* sp.; 29—*Costiniferina arctica*; 30—*Pterospirifer* sp.; 31—*Stenocisma* sp. nov. 1; 32—*Neophricadothyris*; 33—*Stenocisma* sp. nov. 2; 34—*Spiriferella keilhavii*; 35—*D. (D.) mucronata*; 36—indet. echinoconchid; 37—*Lissochonetes superba*; 38—*Rhynchopora kochi*; 39—*Cancrinella spitsbergiana*. Bivalve taxa (right): 1—*Streblopteria winsnesi*; 2—*Vorkutopecten svalbardensis*; 3—*Streblochondria* sp.; 4—*Acanthopecten licharewi*; 5—*Etheripecten* spp.; 6—*Grammatodon* sp.; 7—*Cassianoides sexcostatus*; 8—*Palaeoneilo* sp.; 9—*Grammatodon* (*Cosmetodon*)? *suzuki*; 10—*Palaeolima* sp.; 11—*Atomodesma* sp. 1; 12—*Atomodesma* sp. 2.

followed by recovery of a mixed brachiopod-bivalve assemblage (only found in reworked blocks in Greenland). The age of the boundary between the Wegener Halvø and Schuchert Dal Formations therefore becomes critical to determining whether these seemingly Boreal-wide extinction losses were contemporaneous across the region.

Conodonts extracted from the Ravnefjeld Formation (a black shale unit that is laterally equivalent to the Wegener Halvø Formation) include *Neogondolella rosenkrantzi*, *Xaniognathus abstractus*, and *Merrillina divergens*. Rasmussen et al. (1990) considered this assemblage to be no younger than earliest Capitanian in age, and equivalent to conodonts from the first cycle of the Zechstein Seaway infill of northern Europe. If this is the case, then the top Wegener Halvø level is much older than the Capitanian extinction in Spitsbergen. In contrast, some subsequent studies consider the conodonts (and the basal Zechstein rocks) to be much younger—Wuchiapingian in age—based on the presence of *rosenkrantzi*, now considered a *Mesogondolella* species (e.g., Nielsen and Shen, 2004; Sørensen et al., 2007). This revised age assignment places the top of the Wegener Halvø Formation in the Late Permian, at a level considerably younger than the Capitanian extinction. However, the most recent taxonomic reassessment suggests that the Zechstein *Mesogondolella* species is not *rosenkrantzi* but a younger, derived species (*M. brittanica*), and the true *Mesogondolella rosenkrantzi* of the Ravnefjeld Formation indicates an intra-Capitanian age (Legler and Schneider, 2008). This re-revised age assessment indicates that the brachiopod and bryozoan losses at the top of the Wegener Halvø Formation record a mid- to late Capitanian crisis that can be correlated with the extinction near the 3YLB level in Spitsbergen. This points to a Boreal-wide intra-Capitanian crisis.

There is a similar loss of marine benthic faunal diversity around the Capitanian-Wuchiapingian boundary in the Sverdrup Basin of Arctic Canada. In that location, faunal losses are associated with the near-total disappearance of shallow-marine carbonates (Beauchamp

TABLE 1. PYRITE FRAMBOID SIZE DISTRIBUTIONS FROM FESTNINGEN (FE SAMPLES) AND VAN KEULENHAMNA (VKH SAMPLES)

Sample	Height in section (m)	n	Mean diameter (μm)	Standard deviation	Minimum diameter (μm)	Maximum diameter (μm)
Fe31a*	40.2	7	11.1	3.8	7	16.5
Fe42	47	67	6.8	2.7	2.5	15
Fe44	47.5	128	6.8	3.5	1.5	23.5
Fe45a	47.8	16	10.1	6.5	3.5	32
Fe46a	48.2	44	6.4	2.6	2.5	15.5
Fe51	52	69	6.5	2.4	3	19
Fe59	57.5	27	7.7	3.5	3	16.5
Fe68a	66.2	116	6.1	1.7	3	10.5
Fe70	74	91	5.9	3.8	1.5	23
Fe75	79.5	88	6.2	2.0	3	13
Fe77*	81.5	6	24.2	21.5	5	65
Fe80*	85.5	4	8.6	1.4	7	10
Fe84	88	87	8.9	5.1	2	27.5
VKH63c*	178	1	18	n/a	18	18
VKH68b upper*	185.5	6	10.8	8.7	5.5	28
VKH70b*	189.5	3	11.3	5.9	7	18
VKH70c*	189.8	4	21.4	27.1	6.5	62
VKH72b*	191	6	10.3	2.8	7.5	15.5

Note: n—number of framboids counted per sample.
*Not included in Figure 8 due to small sample size (*n*).

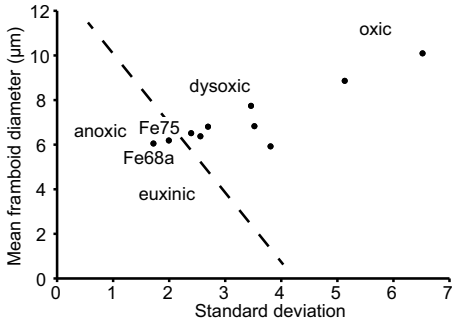

Figure 8. Mean versus standard deviation plot for pyrite-framboid–bearing samples from Kapp Starostin. Most framboidal samples record dysoxic seafloor conditions (the euxinic, anoxic, dysoxic, and oxic fields are based on modern environments) with conditions deteriorating at the extinction level. The most intensely anoxic conditions are seen in beds Fe68a and Fe75, at 66 m and 80 m section height (Fig. 3) respectively. These two levels are immediately either side of the recovery interval.

and Grasby, 2012). The low-diversity survivors, consisting of brachiopods and bryozoans, persisted into the younger Permian, only to disappear in the early Changhsingian (Beauchamp, 1994; Algeo et al., 2012). This left only siliceous sponges in the Sverdrup Basin, but they too soon disappeared (in the late Changhsingian Stage). Thus, the Sverdrup Basin record reveals a very similar three-step diversity decline to that seen in Spitsbergen, with the added benefit of conodont-age control for the younger extinctions. However, the post-Capitanian extinction recovery of brachiopods and bivalves seen in Spitsbergen is not seen in the Sverdrup Basin.

Cause of Capitanian Extinction

The role of marine anoxia in the Capitanian extinction has been put forward (e.g., Clapham and Bottjer, 2007; Clapham et al., 2009). While indeed Isozaki (1997) suggested that a 10-m.y.-long "superanoxic event" in the Panthalassa Ocean began at the Guadalupian-Lopingian boundary, the development of open-ocean anoxia is now known to postdate the intra-Capitanian extinction (Wignall et al., 2010).

There is clear evidence from our combined pyrite petrographic and trace metal study (Figs. 3 and 8) that the intra-Capitanian extinction at Kapp Starostin coincided with a deterioration of seafloor oxygenation, lending support to the anoxia kill hypothesis. However, this redox change is more muted in the shallower-water sections of southern Spitsbergen, and further afield there is little evidence for middle Capitanian anoxia in either the South China sections (Wignall et al., 2009b) or in the Panthalassan accreted terranes of Japan (Wignall et al., 2010). The role of anoxia in the wider Capitanian extinction scenario remains enigmatic, and although it might have played a part at Kapp Starostin, it was probably not the only killer—some other mechanism must have been responsible for losses in southern Spitsbergen where anoxia did not develop.

The extinction level also coincides with the disappearance of carbonates throughout Boreal seas. No limestones are seen above 3YLB in Spitsbergen, nor above the Wegener Halvø Formation in East Greenland, and neither are they developed in the Upper Permian of the Sverdrup Basin. This observation potentially supports ocean acidification as a cause of the Capitanian crisis, at least in higher-latitude regions (e.g., Beauchamp and Grasby, 2012). Due to the greater solubility of CO_2 in colder waters, ocean acidification stresses are more intense at higher latitudes. The observation that extinction losses are very similar amongst brachiopods in China and Spitsbergen would appear to rule out an extinction cause related to temperature alone.

High $\delta^{13}C$ values in the early Capitanian have been interpreted as evidence for a cold climatic episode that drove the Capitanian crisis. Support for this idea came from the observation that only warm-water taxa such as fusulinacean foraminifers were affected (e.g., Isozaki et al., 2007; Kossovaya and Kropatcheva, 2013). However, our discovery of extinction amongst Boreal brachiopods suggests that cold adaptation was of no benefit. Furthermore, a prolonged cooling could be expected to result in the migration of Boreal species into the warmer waters of Panthalassa and Tethys, but this is not observed. Extreme cooling of the magnitude required to cause extinctions would likely result in glacio-eustatic regression, but in Spitsbergen, there is no facies change across the extinction horizon.

Our new data suggest that the Capitanian extinction was of global extent. In South China, the extinction closely coincides with the onset of Emeishan volcanism, suggesting that the deleterious effects of this large igneous province played a key role in the extinction scenario (Wignall et al., 2009a). Volcanically induced effects are multiple and include acidification (from CO_2 release). More subtle volcanogenic killers might include poisoning by trace metals. For example, mercury has been implicated in the Permian-Triassic extinction (Sanei et al., 2012). Short-term cooling caused by volcanic aerosols is another possibility (e.g., Bond et al., 2010b). A proxy for flood basalt volcanism at the level of extinction in Spitsbergen would help to strengthen any volcanism-extinction links.

Recovery and the Transition to Mesozoic Character

Bivalves suffered modest losses during the first Spitsbergen Permian crisis, and the post-extinction interval witnessed a marked increase in molluskan dominance of the shelly benthos, resulting in assemblages more typical of the Mesozoic. This supports the notion of Clapham and Bottjer (2007), who suggested that the tran-

sition from brachiopod- to bivalve-dominated benthos was under way before the start of the Triassic. The aftermath of the Capitanian extinction clearly witnessed some bivalve successes, but the second extinction event in Spitsbergen removed all shelly taxa at some point in the Late Permian.

CONCLUSIONS

Detailed sample collection from Spitsbergen reveals a major brachiopod extinction event from near the top of the Kapp Starostin Formation. This extinction predates the end-Permian mass extinction, because a subsequent recovery of brachiopods and especially bivalves is seen in the Late Permian. This postextinction fauna disappears 10 m below the top of the Kapp Starostin Formation and thus fails to survive until the end of the Permian. The end-Permian extinction in Spitsbergen only eliminated the remaining fauna of siliceous sponges and trace-making organisms. Thus, there are three extinction levels in the Kapp Starostin Formation and one interval of radiation after the oldest extinction.

A combination of Sr isotope, chemostratigraphic, and magnetostratigraphic data suggests that the first and most severe extinction was contemporary with the middle Capitanian mass extinction of lower (Tethyan) latitudes, although further improvements in age dating are needed. Comparison with the record in East Greenland suggests that there was also a major extinction of shelly invertebrates at the top of the Wegener Halvø Formation. Based on conodont dating, this event was likely contemporaneous with the Spitsbergen losses and points to a Boreal-wide crisis in the Middle Permian.

Scenarios involving marine anoxia during the Capitanian extinction are supported by pyrite framboids and trace metal enrichment data from our deepest-water section at Kapp Starostin. However, the extinction is equally severe in the shallower-water sections of southern Spitsbergen, where there is little evidence for anoxia. The crisis also saw the permanent loss of carbonate shelf facies in the region, possibly supporting a role for ocean acidification during the Capitanian crisis, at least in higher, cooler latitudes. The loss of the cool-water invertebrates in Boreal Seas reveals that the Capitanian crisis did not, as previously thought, simply affect tropical marine biota: It was a truly global mass extinction.

ACKNOWLEDGMENTS

This project was supported by funding from the Research Executive Agency (Marie Curie Intra-European Fellowship FP7-PEOPLE-2011-IEF-300455 to D. Bond), and the Natural Environment Research Council (grants NE/J01799X/1 to D. Bond and NE/I015817/1 to P. Wignall). We thank the Norwegian Polar Institute, and in particular Jørn Dybdahl and Monica Sund, for logistical support in the field. Richard Newport at the University of Manchester assisted in cathodoluminescence microscopy. The following were valuable members of the field-work teams: Dan Collins, Tom Goode, Christian Scheibner, and Tom Wignall. We thank Tom Algeo for his constructive review, and Associate Editor Ken MacLeod and Editor Christian Koeberl for their valuable input. This article has been published under the terms of the CC-BY 3.0 license thanks to Gold Open Access funding from the University of Hull.

REFERENCES CITED

Algeo, T., Henderson, C.M., Ellwood, B., Rowe, H., Elswick, E., Bates, S., Lyons, T., Hower, J.C., Smith, C., Maynard, B., Hays, L.E., Summons, R.E., Fulton, J., and Freeman, K.H., 2012, Evidence for a diachronous Late Permian marine crisis from the Canadian Arctic region: Geological Society of America Bulletin, v. 124, p. 1424–1448, doi:10.1130/B30505.1.

Beauchamp, B., 1994, Permian climatic cooling in the Canadian Arctic, *in* Klein, G.D., ed., Pangea: Paleoclimate, Tectonics, and Sedimentation during Accretion, Zenith and Break-Up of a Supercontinent: Geological Society of America Special Paper 288, p. 229–246.

Beauchamp, B., and Grasby, S.E., 2012, Permian lysocline shoaling and ocean acidification along NW Pangea led to carbonate eradication and chert expansion: Palaeogeography, Palaeoclimatology, Palaeoecology, v. 350–352, p. 73–90, doi:10.1016/j.palaeo.2012.06.014.

Blomeier, D.P.G., Dustira, A.M., Forke, H., and Scheibner, C., 2013, Facies analysis and depositional environments of a storm-dominated, temperate to cold, mixed siliceous-carbonate ramp: The Permian Kapp Starostin Formation in NE Svalbard: Norwegian Journal of Geology, v. 93, p. 75–98.

Bond, D.P.G., and Wignall, P.B., 2009, Latitudinal selectivity of foraminifer extinctions during the late Guadalupian crisis: Paleobiology, v. 35, p. 465–483, doi:10.1666/0094-8373-35.4.465.

Bond, D.P.G., and Wignall, P.B., 2010, Pyrite framboid study of marine Permo-Triassic boundary sections: A complex anoxic event and its relationship to contemporaneous mass extinction: Geological Society of America Bulletin, v. 122, p. 1265–1279, doi:10.1130/B30042.1.

Bond, D.P.G., Hilton, J., Wignall, P.B., Ali, J.R., Stevens, L.G., Sun, Y.-D., and Lai, X.-L., 2010a, The Middle Permian (Capitanian) mass extinction on land and in the oceans: Earth-Science Reviews, v. 102, p. 100–116, doi:10.1016/j.earscirev.2010.07.004.

Bond, D.P.G., Wignall, P.B., Wang, W., Izon, G., Jiang, H.-S., Lai, X.-L., Sun, Y.-D., Newton, R.J., Shao, L.-Y., Védrine, S., and Cope, H., 2010b, The mid-Capitanian (Middle Permian) mass extinction and carbon isotope record of South China: Palaeogeography, Palaeoclimatology, Palaeoecology, v. 292, p. 282–294, doi:10.1016/j.palaeo.2010.03.056.

Clapham, M.E., and Bottjer, D.J., 2007, Prolonged Permian–Triassic ecological crisis recorded by molluscan dominance in Late Permian offshore assemblages: Proceedings of the National Academy of Sciences of the United States of America, v. 104, p. 12,971–12,975, doi:10.1073/pnas.0705280104.

Clapham, M.E., Shen, S.-Z., and Bottjer, D.J., 2009, The double mass extinction revisited: Reassessing the severity, selectivity, and causes of the end-Guadalupian biotic crisis (Late Permian): Paleobiology, v. 35, p. 32–50, doi:10.1666/08033.1.

Cohen, K.M., Finney, S.C., Gibbard, P.L., and Fan, J.-X., 2013, The ICS International Chronostratigraphic Chart: Episodes, v. 36, p. 199–204.

Dallmann, W.K., ed., 1999, Lithostratigraphic Lexicon of Svalbard: Review and Recommendations for Nomenclature Use: Upper Palaeozoic to Quaternary Bedrock: Tromsø, Norway, Norsk Polarinstitutt, 318 p.

Dunbar, C.O., 1955, Permian brachiopod faunas of central East Greenland: Meddelelser om Grønland, Udgivne af Kommissionen for Videnskabelige Undersøgelser i Grønland, v. 110, no. 3.

Dustira, A.M., Wignall, P.B., Joachimski, M., Blomeier, D., Hartkopf-Fröder, C., and Bond, D.P.G., 2013, Gradual onset of anoxia across the Permian-Triassic boundary in Svalbard, Norway: Palaeogeography, Palaeoclimatology, Palaeoecology, v. 374, p. 303–313, doi:10.1016/j.palaeo.2013.02.004.

Ehrenberg, S.N., Pickard, N.A.H., Henriksen, L.B., Svana, T.A., Gutteridge, P., and Macdonald, D., 2001, A depositional and sequence stratigraphic model for cold-water, spiculitic strata based on the Kapp Starostin Formation (Permian) of Spitsbergen and equivalent deposits from the Barents Sea: American Association of Petroleum Geologists Bulletin, v. 85, p. 2061–2087, doi:10.1306/8626D347-173B-11D7-8645000102C1865D.

Ehrenberg, S.N., McArthur, J.M., and Thirlwall, M.F., 2010, Strontium isotope dating of spiculitic Permian strata from Spitsbergen outcrops and Barents Sea well-cores: Journal of Petroleum Geology, v. 33, p. 247–254, doi:10.1111/j.1747-5457.2010.00476.x.

Ezaki, Y., and Kawamura, T., 1992, Carboniferous–Permian corals from Skansen & Festningen, Central Spitsbergen: Their faunal characteristics, *in* Nakamura, K., ed., Investigations on the Upper Carboniferous–Upper Permian Succession of West Spitsbergen 1989–1991: Sapporo, Japan, Hokkaido University Press, p. 59–75.

Ezaki, Y., Kawamura, T., and Nakamura, K., 1994, Kapp Starostin Formation in Spitsbergen: A sedimentary and faunal record of Late Permian paleoenvironments in an Arctic region, *in* Embry, A.F., Beauchamp, B., and Glass, D.J., eds., Pangea: Global Environments and Resources: Canadian Society of Petroleum Geologists Memoir 17, p. 647–655.

Gibbs, M.T., Bluth, G.J., Fawcett, P.J., and Kump, L.R., 1999, Global chemical erosion over the last 250 My: Variations due to changes in paleogeography, paleoclimate, and paleogeology: American Journal of Science, v. 299, p. 611–651, doi:10.2475/ajs.299.7-9.611.

Gobbett, D.J., 1964, Carboniferous and Permian brachiopods of Svalbard: Norsk Polarinstitutt Skrifter, v. 127, p. 1–201.

Groves, J.R., and Wang, Y., 2013, Timing and size selectivity of the Guadalupian (Middle Permian) fusulinoidean extinction: Journal of Paleontology, v. 87, p. 183–196, doi:10.1666/12-076R.1.

Gruszczynski, M., Hoffman, A., Małkowski, K., and Veizer, J., 1992, Seawater strontium isotopic perturbation at the Permian-Triassic boundary, West Spitsbergen, and its implications for the interpretation of strontium isotopic data: Geology, v. 20, p. 779–782, doi:10.1130/0091-7613(1992)020<0779:SSIPAT>2.3.CO;2.

Hounslow, M.W., and Nawrocki, J., 2008, Paleomagnetism and magnetostratigraphy of the Permian and Triassic of Spitsbergen: A review of progress and challenges: Polar Research, v. 27, p. 502–522, doi:10.1111/j.1751-8369.2008.00075.x.

Isozaki, Y., 1997, Permo-Triassic boundary superanoxia and stratified superocean: Records from lost deep sea: Science, v. 276, p. 235–238, doi:10.1126/science.276.5310.235.

Isozaki, Y., 2009, Illawarra reversal: The fingerprint of a superplume that triggered Pangean breakup and the end-Guadalupian (Permian) mass extinction: Gondwana Research, v. 15, p. 421–432, doi:10.1016/j.gr.2008.12.007.

Isozaki, Y., Kawahata, H., and Ota, A., 2007, A unique carbon isotope record across the Guadalupian–Lopingian (Middle–Upper Permian) boundary in mid-oceanic paleoatoll carbonates: The high-productivity "Kamura event" and its collapse in Panthalassa: Global and Planetary Change, v. 55, p. 21–38, doi:10.1016/j.gloplacha.2006.06.006.

Jin, Y.-G., Zhang, J., and Shang, Q.-H., 1994, Two phases of the end-Permian mass extinction, *in* Embry, A.F., Beauchamp, B., and Glass, D.J., eds., Pangea: Global Environments and Resources: Canadian Society of Petroleum Geologists Memoir 17, p. 813–822.

Jost, A.B., Mundil, R., He, B., Brown, S.T., Altiner, D., Sun, Y.-D., DePaolo, D.J., and Payne, J.L., 2014, Constrain-

ing the cause of the end-Guadalupian extinction with coupled records of carbon and calcium isotopes: Earth and Planetary Science Letters, v. 396, p. 201–212, doi:10.1016/j.epsl.2014.04.014.

Kani, T., Fukui, M., Isozaki, Y., and Nohda, S., 2008, The Paleozoic minimum of $^{87}Sr/^{86}Sr$ ratio in the Capitanian (Permian) mid-oceanic carbonates: A critical turning point in the late Paleozoic: Journal of Asian Earth Sciences, v. 32, p. 22–33, doi:10.1016/j.jseaes.2007.10.007.

Kani, T., Hisanabe, C., and Isozaki, Y., 2013, The Capitanian (Permian) minimum of $^{87}Sr/^{86}Sr$ ratio in the mid-Panthalassan paleo-atoll carbonates and its demise by the deglaciation and continental doming: Gondwana Research, v. 24, p. 212–221, doi:10.1016/j.gr.2012.08.025.

Kobayashi, F., 1997, Middle Permian biogeography based on fusulinacean faunas, *in* Ross, C.A., Ross, J.R.P., and Brenckle, P.L., eds., Late Paleozoic Foraminifera: Their Biogeography, Evolution, and Paleoecology; and the Mid-Carboniferous Boundary: Cushman Foundation for Foraminiferal Research Special Publication 36, p. 73–76.

Korte, C., Jasper, T., Kozur, H.W., and Veizer, J., 2006, $^{87}Sr/^{86}Sr$ record of Permian seawater: Palaeogeography, Palaeoclimatology, Palaeoecology, v. 240, p. 89–107, doi:10.1016/j.palaeo.2006.03.047.

Kossovaya, O.L., and Kropatcheva, G.S., 2013, Extinction of Guadalupian rugose corals: An example of biotic response to the Kamura event (southern Primorye, Russia), *in* Gąsiewicz, A., and Słowakiewicz, M., eds., Palaeozoic Climate Cycles: Their Evolutionary and Sedimentological Impact: Geological Society of London Special Publication 376, doi:10.1144/SP376.132013.

Legler, B., and Schneider, J.W., 2008, Marine ingressions into the Middle/Late Permian saline lake of the southern Permian Basin (Rotliegend, northern Germany) possibly linked to sea-level highstands in the Arctic rift system: Palaeogeography, Palaeoclimatology, Palaeoecology, v. 267, p. 102–114, doi:10.1016/j.palaeo.2008.06.009.

McArthur, J.M., Donovan, D.T., Thirwall, M.F., Fouke, B.W., and Mattey, D., 2000, Strontium isotope profile of the early Toarcian (Jurassic) oceanic anoxic event, the duration of ammonite biozones, and belemnite palaeotemperatures: Earth and Planetary Science Letters, v. 179, p. 269–285, doi:10.1016/S0012-821X(00)00111-4.

McArthur, J.M., Howarth, R.J., and Bailey, T.R., 2001, Strontium isotope stratigraphy: LOWESS Version 3: Best fit to the marine Sr-isotope curve for 0–509 Ma and accompanying look-up table for deriving numerical age: The Journal of Geology, v. 109, p. 155–170, doi:10.1086/319243.

Nakrem, H.A., 1994, Environmental distribution of bryozoans in the Permian of Spitsbergen, *in* Hayward, P.J., Ryland, J.S., and Taylor, P.D., eds., Proceedings of the 9th International Bryozoology Conference, Swansea, 1992: Fredensborg, Denmark, Olsen and Olsen, p. 133–137.

Nawrocki, J., and Grabowski, J., 2000, Palaeomagnetism of Permian through Early Triassic sequence in central Spitsbergen: Contribution to magnetostratigraphy: Geological Quarterly, v. 44, p. 109–117.

Nielsen, J.K., and Shen, Y., 2004, Evidence for sulfidic deep water during the Late Permian in the East Greenland Basin: Geology, v. 32, p. 1037–1040, doi:10.1130/G20987.1.

Rasmussen, J.A., Piasecki, S., Stemmerik, L., and Stouge, S., 1990, Late Permian conodonts from central east Greenland: Neues Jahrbuch für Geologie und Palaontologie, Abhandlungen, v. 178, p. 309–324.

Sanei, H., Grasby, S.E., and Beauchamp, B., 2012, Latest Permian mercury anomalies: Geology, v. 40, p. 63–66, doi:10.1130/G32596.1.

Shen, S.-Z., and Shi, G.-R., 1996, Diversity and extinction patterns of Permian brachiopods of South China: Historical Biology, v. 12, p. 93–110, doi:10.1080/08912969609386558.

Shen, S.-Z., and Shi, G.-R., 2004, Capitanian (late Guadalupian, Permian) global brachiopod palaeobiogeography and latitudinal diversity pattern: Palaeogeography, Palaeoclimatology, Palaeoecology, v. 208, p. 235–262, doi:10.1016/j.palaeo.2004.03.009.

Sørensen, A.M., Håkansson, E., and Stemmerik, L., 2007, Faunal migration into the Late Permian Zechstein basin—Evidence from bryozoan palaeobiogeography: Palaeogeography, Palaeoclimatology, Palaeoecology, v. 251, p. 198–209, doi:10.1016/j.palaeo.2007.03.045.

Stanley, S.M., and Yang, X., 1994, A double mass extinction at the end of the Paleozoic Era: Science, v. 266, p. 1340–1344, doi:10.1126/science.266.5189.1340.

Stemmerik, L., 2001, Stratigraphy of the Upper Permian Wegener Halvø Formation, Karstryggen area, East Greenland—A low productivity carbonate platform: Sedimentology, v. 48, p. 79–97, doi:10.1046/j.1365-3091.2001.00352.x.

Stemmerik, L., and Worsley, D., 2005, 30 years on—Arctic Upper Palaeozoic stratigraphy, depositional evolution and hydrocarbon prospectivity: Norwegian Journal of Geology, v. 85, p. 151–168.

Suits, N.S., and Wilkin, R.T., 1998, Pyrite formation in the water column and sediment of a meromictic lake: Geology, v. 26, p. 1099–1102, doi:10.1130/0091-7613(1998)026<1099:PFITWC>2.3.CO;2.

Wang, W., Cao, C.-Q., and Wang, Y., 2004, The carbon isotope excursion on GSSP candidate section of Lopingian-Guadalupian boundary: Earth and Planetary Science Letters, v. 220, p. 57–67, doi:10.1016/S0012-821X(04)00033-0.

Wignall, P.B., Morante, R., and Newton, R., 1998, The Permo-Triassic transition in Spitsbergen: $\delta^{13}C_{org}$ chemostratigraphy, Fe and S geochemistry, facies, fauna and trace fossils: Geological Magazine, v. 135, p. 47–62, doi:10.1017/S0016756897008121.

Wignall, P.B., Sun, Y.-D., Bond, D.P.G., Izon, G., Newton, R.J., Védrine, S., Widdowson, M., Ali, J.R., Lai, X.-L., Jiang, H.-S., Cope, H., and Bottrell, S.H., 2009a, Volcanism, mass extinction, and carbon isotope fluctuations in the Middle Permian of China: Science, v. 324, p. 1179–1182, doi:10.1126/science.1171956.

Wignall, P.B., Vedrine, S., Bond, D.P.G., Wang, W., Lai, X.L., Ali, J.R., and Jiang, H.S., 2009b, Facies analysis and sea-level change at the Guadalupian-Lopingian global stratotype (Laibin, South China), and its bearing on the end-Guadalupian mass extinction: Journal of the Geological Society of London, v. 166, p. 655–666, doi:10.1144/0016-76492008-118.

Wignall, P.B., Bond, D.P.G., Kuwahara, K., Kakuwa, Y., Newton, R.J., and Poulton, S.W., 2010, An 80 million year oceanic redox history from Permian to Jurassic pelagic sediments of the Mino-Tamba terrane, SW Japan, and the origin of four mass extinctions: Global and Planetary Change, v. 71, p. 109–123, doi:10.1016/j.gloplacha.2010.01.022.

Wignall, P.B., Bond, D.P.G., Newton, R.J., Haas, J., Hips, K., Wang, W., Jiang, H.-S., Lai, X.-L., Sun, Y.-D., Altiner, D., Védrine, S., and Zajzon, N., 2012, The Capitanian (Middle Permian) mass extinction in western Tethys: A fossil, facies and $\delta^{13}C$ study from Hungary and Hydra Island (Greece): Palaios, v. 27, p. 78–89, doi:10.2110/palo.2011.p11-058r.

Wilkin, R.T., and Barnes, H.L., 1997, Formation processes of framboidal pyrite: Geochimica et Cosmochimica Acta, v. 61, p. 323–339, doi:10.1016/S0016-7037(96)00320-1.

Wilkin, R.T., Barnes, H.L., and Brantley, S.L., 1996, The size distribution of framboidal pyrite in modern sediments: An indicator of redox conditions: Geochimica et Cosmochimica Acta, v. 60, p. 3897–3912, doi:10.1016/0016-7037(96)00209-8.

Yang, X.-N., Shi, G.-J., Liu, J.-R., Chen, Y.-T., and Zhou, J.-P., 2000, Inter-taxa differences in extinction process of Maokouan (Middle Permian) fusulinaceans: Science in China, ser. D, v. 43, p. 633–637, doi:10.1007/BF02879507.

Zhou, L., Wignall, P.B., Su, J., Xie, S.-C., Zhao, L.-S., and Huang, J.-H., 2012, U/Mo ratios and $\delta^{98/95}Mo$ as local and global redox proxies during mass extinction events: Chemical Geology, v. 324–325, p. 99–107, doi:10.1016/j.chemgeo.2012.03.020.

Science Editor: Christian Koeberl
Associate Editor: Kenneth G. MacLeod

Manuscript Received 7 October 2014
Revised Manuscript Received 27 January 2015
Manuscript Accepted 4 March 2015

Printed in the USA